Extracellular protons titrate voltage gating of a ligand-gated ion channel

Juan Ramón Martínez-François, Yanping Xu, and Zhe Lu

Department of Physiology, Howard Hughes Medical Institute, University of Pennsylvania, Philadelphia, PA 19104

Cyclic nucleotide–gated channels mediate transduction of light into electric signals in vertebrate photoreceptors. These channels are primarily controlled by the binding of intracellular cyclic GMP (cGMP). Glutamate residue 363 near the extracellular end of the ion selectivity filter interacts with the pore helix and helps anchor the filter to the helix. Disruption of this interaction by mutations renders the channels essentially fully voltage gated in the presence of saturating concentrations of cGMP. Here, we find that lowering extracellular pH makes the channels conduct in an extremely outwardly rectifying manner, as does a neutral glutamine substitution at E363. A pair of cysteine mutations, E363C and L356C (the latter located midway the pore helix), largely eliminates current rectification at low pH. Therefore, this low pH-induced rectification primarily reflects voltage-dependent gating involving the ion selectivity filter rather than altered electrostatics around the external opening of the ion pore and thus ion conduction. It then follows that protonation of E363, like the E363Q mutation, disrupts the attachment of the selectivity filter to the pore helix. Loosening the selectivity filter from its surrounding structure shifts the gating equilibrium toward closed states. At low extracellular pH, significant channel opening occurs only when positive voltages drive the pore from a low probability open conformation to a second open conformation. Consequently, at low extracellular pH the channels become practically fully voltage gated, even in the presence of a saturating concentration of cGMP.

The Journal of General Physiology

INTRODUCTION

CNG channels mediate the transduction of light signals to electrical signals in vertebrate photoreceptors. These channels open upon binding intracellular cGMP (Stryer, 1986; Yau and Baylor, 1989; Kaupp and Seifert, 2002; Matulef and Zagotta, 2003; Fu and Yau, 2007; Biel and Michalakis, 2009). The intracellular cGMP concentration is elevated in darkness, and the opening of CNG channels depolarizes the photoreceptor membrane. Light indirectly lowers the intracellular cGMP concentration, thereby closing the channels and hyperpolarizing the photoreceptors. To accomplish this transduction faithfully, CNG channels must be tightly controlled by intracellular cGMP.

Activity of CNG channels is sensitive to extracellular pH (pH_o) (Goulding et al., 1992; Root and MacKinnon, 1994). A glutamate residue near the external end of the selectivity filter has been identified as the protonation site because replacing it by a neutral residue eliminates pH_o sensitivity in the olfactory CNGA2 channel. Titrating the site reveals various channel states, a phenomenon that has been interpreted in terms of variations in ion conduction (Root and MacKinnon, 1994). Additionally, in the retinal CNGA1 channel, neutral mutations at the corresponding glutamate residue, E363, were shown to render the macroscopic I-V curve outwardly rectifying (Root and MacKinnon, 1993; Eismann et al., 1994; Sesti et al., 1995), a phenomenon that is intuitively consistent with, and had thus been attributed primarily to, alterations in the channel's conduction properties. We have recently found that mutations at E363 in CNGA1 render the I-V curve rectifying primarily by dramatically enhancing the wild-type channel's inherent mild voltage sensitivity (Martínez-François et al., 2009). The dramatically enhanced voltage sensitivity does not appear to originate from the positively charged fourth transmembrane segment that functions as the primary voltage sensor in classical voltage-gated ion channels, but rather from the ion selectivity filter region. The following observations offer clues as to the mechanism by which E363 mutations accentuate voltage gating. Mutations at both E363 and Y352 (the latter located in the pore helix) enhance channel voltage sensitivity but in a non-additive manner. Therefore, E363 interacts with the pore helix likely by forming a hydrogen bond. Conceivably, such interaction helps to properly anchor the external end of the selectivity filter. Disrupting this interaction by substituting neutral residues at E363 apparently renders the channels practically fully voltage gated, even in the presence of saturating concentrations of cGMP. Consistent with this interpretation, other

Correspondence to Zhe Lu: zhelu@mail.med.upenn.edu

Abbreviations used in this paper: DTT, dithiothreitol; GO, glucose oxidase.

© 2010 Martínez-François et al. This article is distributed under the terms of an Attribution–Noncommercial–Share Alike–No Mirror Sites license for the first six months after the publication date (see http://www.rupress.org/terms). After six months it is available under a Creative Commons License (Attribution–Noncommercial–Share Alike 3.0 Unported license, as described at http://creativecommons.org/licenses/by-nc-sa/3.0/).

The Rockefeller University Press $30.00
J. Gen. Physiol. Vol. 136 No. 2 179–187
www.jgp.org/cgi/doi/10.1085/jgp.201010444

Downloaded from http://rupress.org/jgp/article-pdf/136/2/179/1788741/jgp_201010444.pdf by guest on 11 February 2026

mutations in the region around the ion selectivity filter produce similar phenotypes. Mutations at E363 that render CNG channels gated by voltage shift the channels' gating equilibrium toward closed conformations. Channel open probability increases when depolarization drives the channel pore from a low probability open conformation toward a second open conformation. Evidently, the structure surrounding the selectivity filter has evolved to hold the filter "firmly" in place and thereby suppress significant expression of the inherent voltage-dependent gating of CNGA1. Additionally, some mutations around the selectivity filter cause the channel to exhibit desensitization to cGMP (Mazzolini et al., 2009).

Here, we find that lowering pH_o renders CNGA1 channels voltage gated in the presence of a saturating concentration of cGMP. We set out to investigate the underlying mechanism.

MATERIALS AND METHODS

Molecular biology and oocyte preparation

Complementary DNA for CNGA1 (Kaupp et al., 1989) was cloned into the pGEM-HE plasmid (Liman et al., 1992), which was

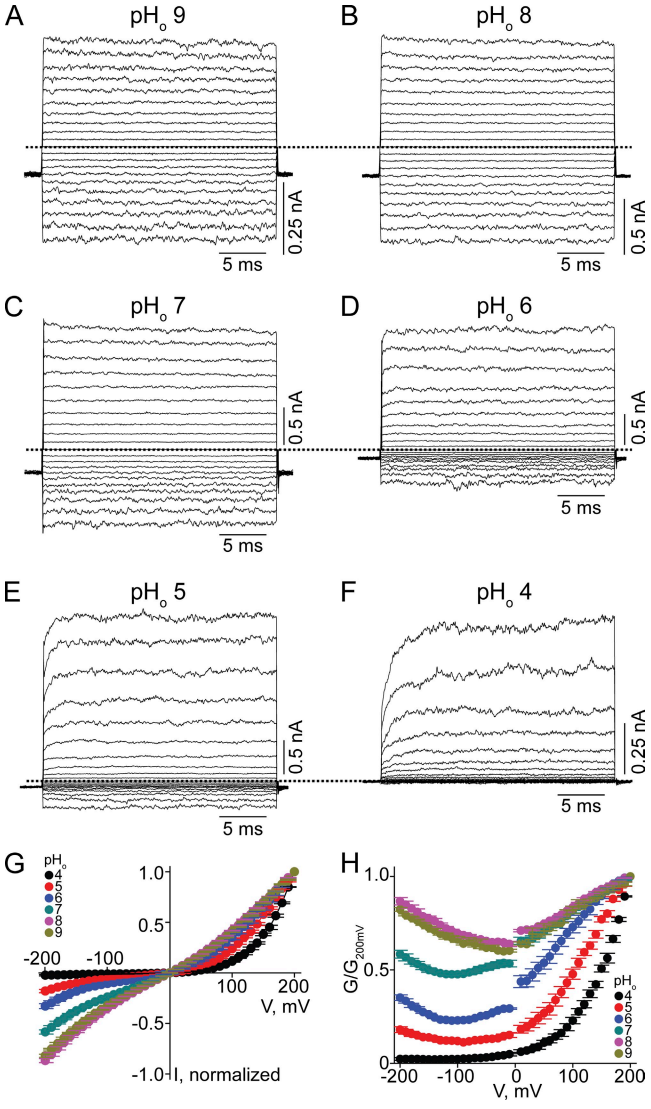

Figure 1. Extracellular protons render the CNGA1 channel voltage sensitive in HEPES-buffered solutions. (A–F) Macroscopic current traces at the indicated pH_o and fixed pH_i 8, recorded in symmetric 130 mM Na^+ and 2 mM of intracellular cGMP from inside-out patches containing CNGA1 channels. Currents were elicited by stepping from the −80-mV holding potential to voltages between −200 and 200 mV in 10-mV increments. Only traces every 20 mV are shown for clarity. Dotted lines indicate zero current level. (G) I-V curves (mean ± SEM; $n = 5$) at the indicated pH_o, each normalized to the current at 200 mV. (H) Corresponding normalized G-V curves (mean ± SEM; $n = 5$).

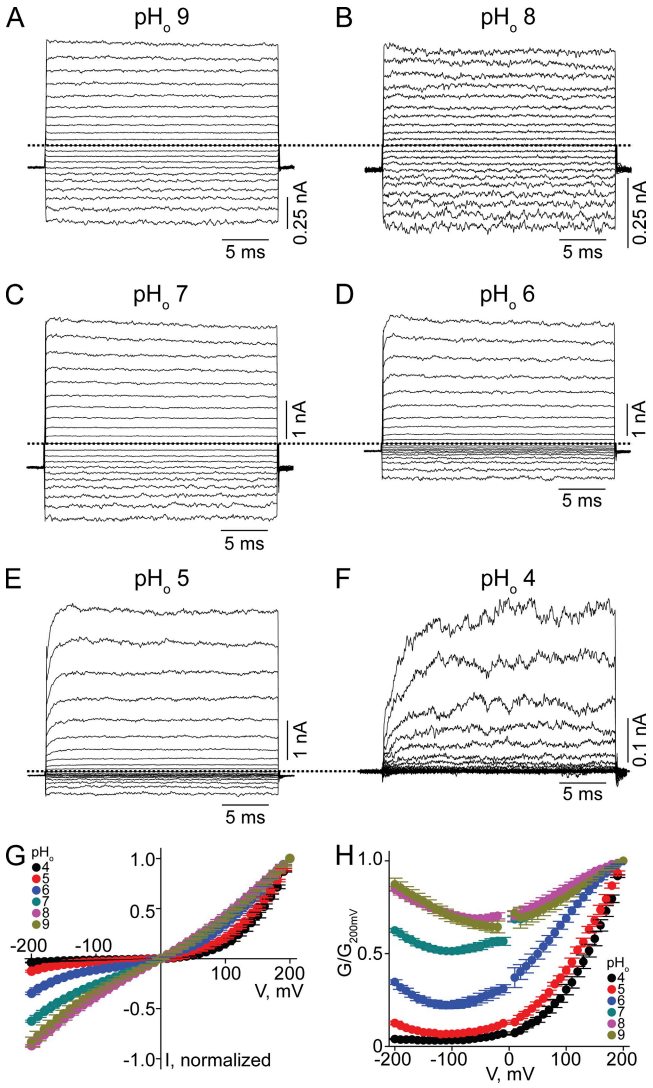

Figure 2. Extracellular protons render the CNGA1 channel voltage sensitive in phosphate-buffered solutions. (A–F) Macroscopic current traces at the indicated pH_o and fixed pH_i 8, recorded in symmetric 130 mM Na^+ and 2 mM of intracellular cGMP from inside-out patches containing CNGA1 channels. (G) I-V curves (mean ± SEM; $n = 5$) at the indicated pH_o, each normalized to the current at 200 mV. (H) Corresponding normalized G-V curves (mean ± SEM; $n = 5$).

Downloaded from http://rupress.org/jgp/article-pdf/136/2/179/1788741/jgp_201010444.pdf by guest on 11 February 2026

provided by S. Siegelbaum (Columbia University, New York, NY). Mutant cDNAs were obtained through PCR-based mutagenesis and confirmed by DNA sequencing. The cRNAs were synthesized with T7 polymerase (Promega) using linearized cDNA as a template. Oocytes harvested from *Xenopus laevis* were incubated in a solution containing (in mM): 82.5 NaCl, 2.5 KCl, 1.0 $MgCl_2$, 5.0 HEPES, pH 7.6, and 2–4 mg/ml collagenase (Worthington Biochemical Corporation). The oocyte preparation was agitated at 100 rpm for 40–60 min. It was then rinsed thoroughly and stored in a solution containing (in mM): 96 NaCl, 2.5 KCl, 1.8 $CaCl_2$, 1.0 $MgCl_2$, 5 HEPES, pH 7.6, and 50 µg/ml gentamicin. Defolliculated oocytes were selected and injected with RNA at least 2 and 16 h, respectively, after collagenase treatment. All oocytes were stored at 18°C.

Recordings and solutions

Currents were recorded from inside-out membrane patches of *Xenopus laevis* oocytes previously injected with the desired cRNA using an amplifier (Axopatch 200B; MDS Analytical Technologies). Macroscopic currents were filtered at 5 kHz and sampled at 50 kHz using an analogue-to-digital converter (Digidata 1322A; MDS Analytical Technologies) interfaced to a personal computer. pClamp 8 software (MDS Analytical Technologies) was used for amplifier control and data acquisition. Wild-type and mutant channels were activated with a saturating concentration (2 mM) of intracellular cGMP, and unless specified otherwise, the currents were elicited by stepping the voltage from the −80-mV holding potential to voltages between −200 and 200 mV in 10-mV increments. Currents in the absence of cGMP were used as template for subsequent offline background current corrections. The background currents were 56.80 ± 5.63 pA at 200 mV and −50.70 ± 5.81 pA at −200 mV ($n = 10$), comparable to those of uninjected oocytes. Except where specified, phosphate-buffered solutions were used to perform all patch clamp recordings. The solutions contained (in mM): 0.1 EDTA, 10 "Na_2HPO_4 + NaH_2PO_4" in a ratio yielding the specified pH, and sufficient NaCl to bring total Na^+ concentration to 130 mM. HEPES-buffered solutions contained (in mM): 130 NaCl, 0.1 EDTA, and 5 HEPES; pH was adjusted with NaOH or HCl. To examine potential isotope effects, D_2O was used instead of H_2O to make recording solutions. For H_2O_2 experiments, oocytes were incubated before patch recording in storage solution either with 10 mM H_2O_2 for 2 h or with 10 mU/ml glucose oxidase (GO) and 5 mM glucose for 16–24 h. For dithiothreitol (DTT) experiments, oocytes were incubated before patch recording for 30 min in storage solution containing 20 mM DTT. All chemicals were purchased from Sigma-Aldrich.

Data analysis

G-V curves were calculated by dividing the steady-state current value at each voltage by the electrochemical driving force, and then normalizing to the value at 200 mV. Data analysis and curve fitting were performed with Origin 8.0 (OriginLab Corp.). Molecular models were prepared with PyMOL 1.0 (DeLano Scientific). The figures were made with Origin 8.0 (OriginLab Corp.) and Illustrator CS4 (Adobe Systems Inc.).

RESULTS

Extracellular, not intracellular, protons titrate voltage sensitivity of CNGA1 channels

We first examined the effect of varying pH_o on CNGA1 macroscopic currents activated by a saturating concentration of cGMP, while intracellular pH (pH_i) was kept

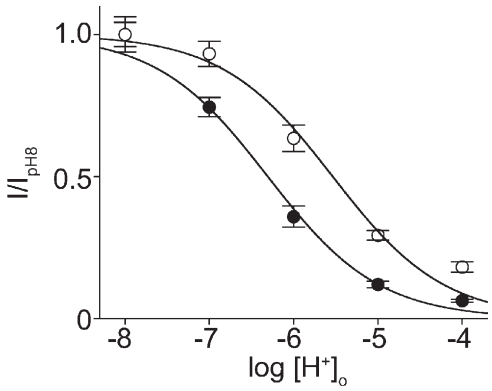

Figure 3. Current inhibition by extracellular protons. Fraction of current relative to that at pH_o 8 (I/I_{pH8}; mean ± SEM; $n = 5$), plotted against pH_o for 50 mV (open circles) and −50 mV (filled circles). Curves are Hill equation fits with a common coefficient (n) yielding $IC_{50} = 4.9 \pm 1.2 \times 10^{-7}$ M at −50 mV ($pK_a = 6.3$), $IC_{50} = 2.9 \pm 0.7 \times 10^{-6}$ M at 50 mV ($pK_a = 5.5$), and $n = 0.66 \pm 0.06$.

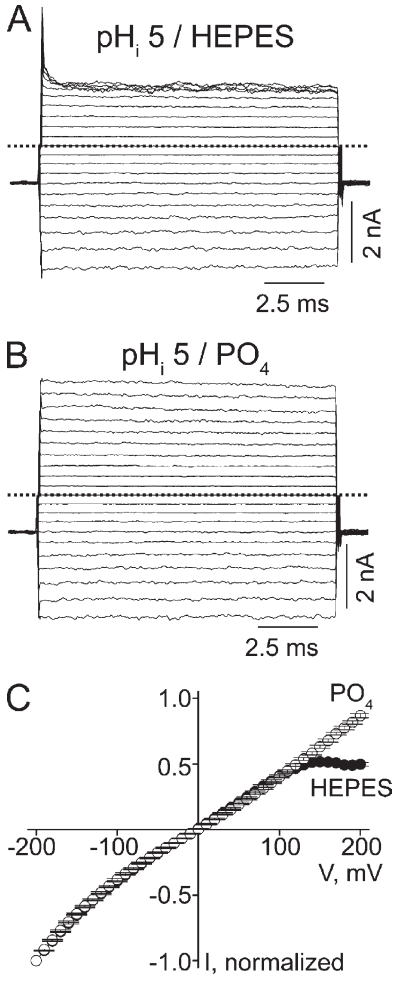

Figure 4. Voltage-dependent CNGA1 block in HEPES- or phosphate-buffered solutions at pH_i 5. (A) Macroscopic currents at pH_i 5 and pH_o 8, recorded in HEPES-buffered solution. (B) Macroscopic currents at pH_i 5 and pH_o 8, recorded in phosphate-buffered solutions. (C) Mean I-V curves (mean ± SEM; $n = 5$) determined at the end of the test pulses in the presence of HEPES- or phosphate-buffered solutions.

Downloaded from http://rupress.org/jgp/article-pdf/136/2/179/1788741/jgp_201010444.pdf by guest on 11 February 2026

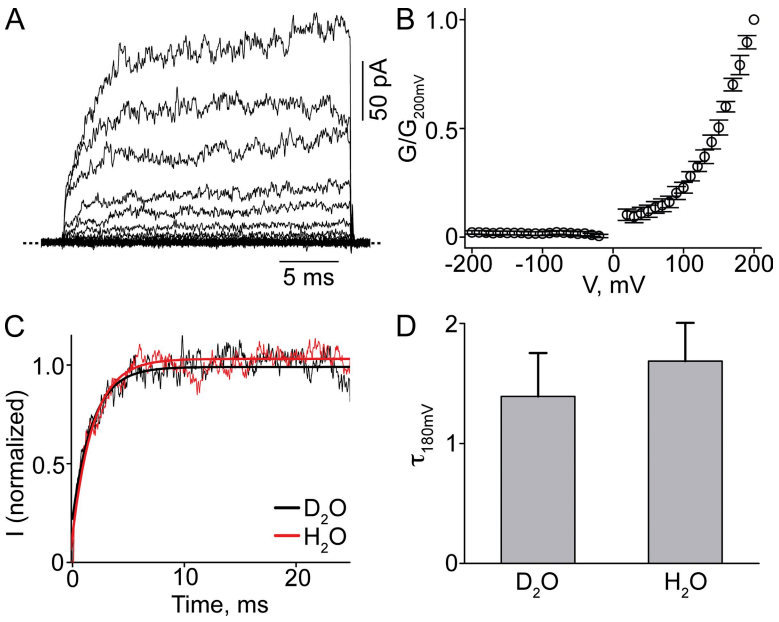

Figure 5. Effect of D_2O on CNGA1 current at pH_o 4. (A and B) Macroscopic currents at pH_o 4 (A) and corresponding G-V curve (B; mean ± SEM; n = 4) for the wild-type CNGA1 channel in D_2O solutions. (C) Current transients elicited by stepping membrane voltage from −80 to 180 mV in D_2O (from A; black) or H_2O (from Fig. 2 F; red). The superimposed curves are single-exponential fits. (D) Time constant (mean ± SEM; n = 4) for current activation at 180 mV (τ_{180mV}) in D_2O and H_2O solutions obtained from fits as shown in C.

at 8.0 (Fig. 1). At high pH_o (Fig. 1, A–C) currents develop instantaneously after voltage jumps, and the channels exhibit approximately linear I-V curves (Fig. 1 G). As pH_o was lowered, current developed more slowly and became suppressed, inward current much more so than outward current (Fig. 1, D–F). Consequently, the I-V curves exhibit outward rectification (Fig. 1 G). To further illustrate the voltage sensitivity of macroscopic conductance, we calculated the conductance from the current/electrochemical driving force ratio and plotted it against voltage (Fig. 1 H). The channels become largely voltage gated at pH_o 4 (Fig. 1, F and H). In these experiments, we used HEPES as buffer. Because commercial HEPES contains a minute amount of contaminants that may block ion channels (Guo and Lu, 2000, 2002), we also performed the above experiments using phosphate as buffer (Fig. 2). Both conditions yielded comparable results (Figs. 1 and 2).

Fig. 3 plots the fraction of current at various pH_o for 50 and −50 mV, relative to current at pH_o 8. Lowering pH_o profoundly suppresses the current, and the apparent pK_a for inhibition is lowered with depolarization. Therefore, at positive voltages, a lower pH_o is required to suppress the current; at low pH_o, a more positive voltage is required to open the channels (Fig. 2 H).

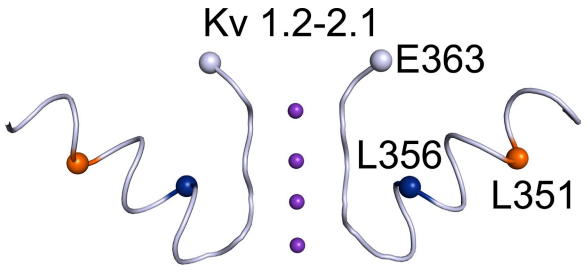

Figure 6. Partial crystal structure model of the Kv1.2-2.1 chimeric K^+ channel (PDB 2R9R) featuring the pore helix and the selectivity filter in two diagonally opposite subunits. Residue numbers are those of the corresponding residues in CNGA1.

It has been reported that in the presence of cAMP or subsaturating concentrations of cGMP, CNGA1 activity is affected by pH_i (Picco et al., 1996; Gavazzo et al., 1997). We thus examined whether pH_i also affects CNGA1 activity under our experimental conditions. While keeping pH_o at 8.0, lowering pH_i to 5 does not significantly affect inward current but suppresses outward current at extreme positive voltages (Fig. 4 A), rendering the I-V curve inwardly rectifying (Fig. 4 C). This latter effect only occurs in HEPES-, not phosphate-, buffered solutions (Fig. 4, B and C). The rectification must therefore reflect voltage-dependent channel block by contaminants in HEPES-buffered solutions. For this reason, all experiments described below were performed in the presence of phosphate-buffered solutions on both sides of the membrane. The above results are in line with the finding of Gavazzo et al. (1997) that altering pH_i does not significantly affect CNGA1 activity at saturating cGMP.

The rather slow time course of current development at low pH_o suggests that the apparent voltage sensitivity likely reflects proton-induced conformational changes. That is, kinetics of current development are limited by a transition downstream from protonation. If so, the kinetics should not be significantly affected in deuterium oxide (D_2O) (Jencks, 1987; Root and MacKinnon, 1994; Lu and MacKinnon, 1995). Indeed, exposing the channels to D_2O did not slow the kinetics of current onset; the G-V curve is unaffected, as expected for an equilibrium property (Fig. 5).

Downloaded from http://rupress.org/jgp/article-pdf/136/2/179/1788741/jgp_201010444.pdf by guest on 11 February 2026

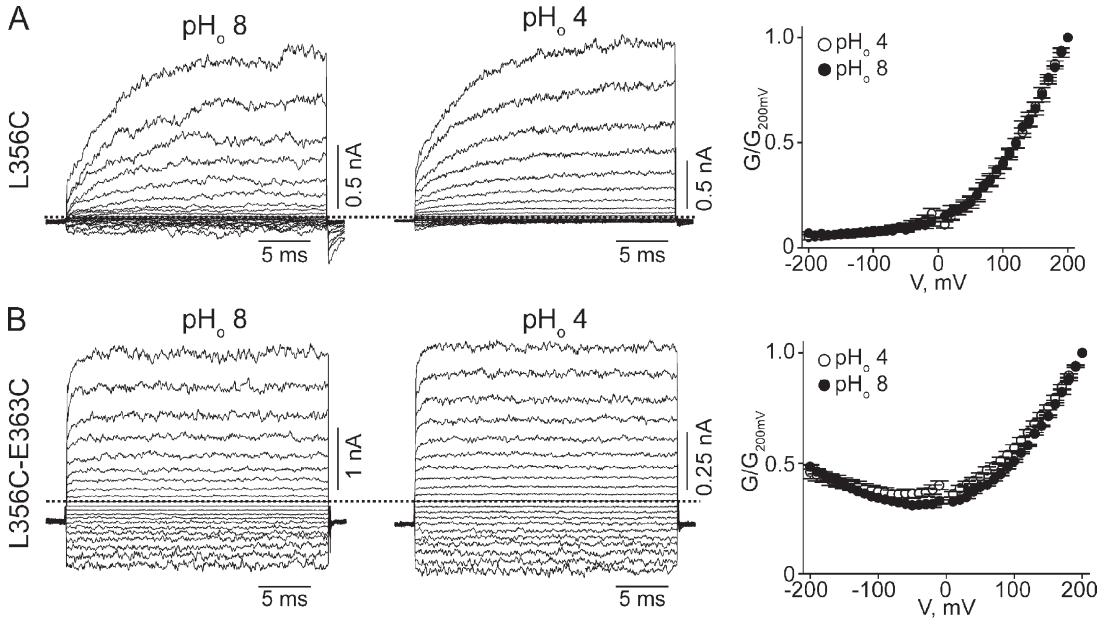

Figure 7. Effects of cysteine mutations at L356 and E363 on proton and voltage sensitivity of CNGA1 channels. (A and B) Macroscopic currents at pH_o 8 (left) or 4 (middle) for the L356C (A) or L356C-E363C (B) mutants, and the corresponding G-V curves (right; mean ± SEM; $n = 5$).

Effects of double-cysteine mutations on proton and voltage sensitivity of CNGA1 channels

E363 appears to form, with a residue in the pore helix, a hydrogen bond that suspends the selectivity filter in such a manner that in the presence of a saturating concentration of cGMP, the filter adopts a conductive conformation independent of voltage (Martínez-François et al., 2009). We surmise that when this hydrogen bond is disrupted by lowering pH_o, the selectivity filter is no longer properly anchored and requires a positive voltage to help stabilize it in a conductive conformation.

To test this possibility, we tried to engineer interacting cysteine pairs at residue 363 and in the pore helix. E363C mutant channels express no detectable current. We then mutated the 12 residues (^{347}YVYSLYWSTLTL^{358}) within the pore helix of the E363C mutant channel, one at a time, to cysteine. Two double-cysteine mutants, L351C-E363C and L356C-E363C, expressed sufficient macroscopic current for examination. For visual reference, we mapped the relevant CNGA1 residues onto the structure (Long et al., 2007) of the Kv1.2-2.1 chimeric channel (Fig. 6).

CNGA1 channels containing a single L356C mutation exhibit pronounced voltage sensitivity but little pH_o sensitivity (Fig. 7 A). This finding suggests that the L356C mutation by itself disrupts proper attachment of the selectivity filter. In contrast, the L356C-E363C double-mutant channels exhibit little voltage or pH_o sensitivity (compare Fig. 7 B with Fig. 2). On the basis of the Kv1.2-2.1 structure (Fig. 6) (Long et al., 2007), residue 356 is on the side of the pore helix facing residue 363; hence, formation of a disulfide bond between them is possible. Given its location, the potential disulfide bond would be buried inside the channel protein. We hope that over a relatively long exposure, some DTT molecules in the extracellular solution may be able to penetrate into the protein to open the disulfide bond in a small yet detectable fraction of channels. Indeed, exposing the channels to extracellular DTT for 30 min causes a significant, if modest, reduction in the degree of rectification in L356C-E363C double-mutant channels (Fig. 8 A), namely, a 22.4 ± 1.2% ($n = 5$) reduction in the ratio of currents at −200 and at 200 mV (I_{-200}/I_{200}), compared with the control (Fig. 8 D). This finding is consistent with DTT treatment reducing the disulfide bond in a fraction of channels. After exposure to extracellular H_2O_2, the channels' conductance at −200 mV approached that at 200 mV (compare Fig. 8 B with Fig. 7 B), leading to an increase in I_{-200}/I_{200} (Fig. 8 D). Indistinguishable results were obtained whether H_2O_2 was added directly to the extracellular solution (Fig. 8, B and D) or generated locally using the enzyme GO (Fig. 8, C and D). These results are consistent with the possibility that in some channels, the cysteine pair(s) has not spontaneously formed a disulfide bond before the above maneuvers.

As for the L351C channels, they exhibit, like wild type, little voltage sensitivity at high pH_o but strong sensitivity at low pH_o (Fig. 9 A). Therefore, the L351C mutation by itself does not appear to alter the attachment of the selectivity filter. The L351C-E363C channels, however, exhibit voltage sensitivity at both high and low pH_o (Fig. 9 B), a phenotype shared by many mutants with neutral substitutions at E363. According to the Kv1.2-2.1 structure, residue 351 would be located on the side of the pore helix facing away from E363 (Fig. 6). Thus, the L351C mutation seems

Downloaded from http://rupress.org/jgp/article-pdf/136/2/179/1788741/jgp_201010444.pdf by guest on 11 February 2026

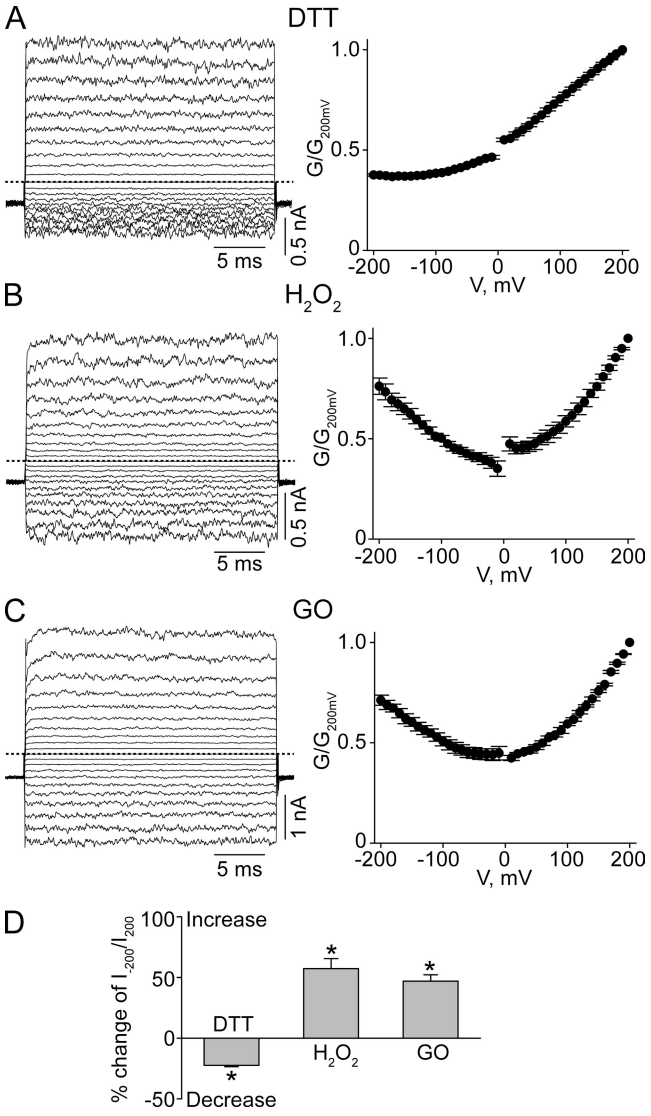

Figure 8. Effects of DTT or H_2O_2 on L356C-E363C double-mutant channels. (A–C) Macroscopic currents at pH_o 8 (left) and corresponding G-V curves (right; mean ± SEM; $n = 5$) for L356C-E363C mutant channels after the application of DTT (A), H_2O_2 (B), or GO (C). (D) Percent change of I_{-200}/I_{200} values (mean ± SEM; $n = 5$) at pH_o 8 of the L356C-E363C double-mutant channels after exposure to the reagents indicated. Positive or negative changes signify increases or decreases in the I_{-200}/I_{200} value, respectively. *, $P < 0.001$ (one-way ANOVA) with respect to the control mean.

to simply rescue the E363C mutant but does not appear to form a disulfide bond with E363C. Consistent with the latter possibility, the shape of the G-V curve of L351C-E363C mutant channels was not significantly affected by either DTT or H_2O_2 (Fig. 10).

DISCUSSION

We find that extracellular protons titrate CNGA1's voltage sensitivity in such a manner that lowering pH_o renders the channels practically fully gated by voltage, even in the presence of saturating concentrations of cGMP. The voltage sensitivity of wild-type channels at low pH_o resembles that of mutants with a neutral residue at E363 near the external end of the selectivity filter (Martínez-François et al., 2009). The E363 mutations have been shown to disrupt a hydrogen bond between E363 and probably Y352 in the pore helix. Here, we find that extracellular protons titrate this hydrogen bond, tuning the apparent voltage sensitivity of CNGA1 channels. In fact, a pair of cysteine mutations, E363C and L356C, apparently "locks" the selectivity filter in a conductive conformation that exhibits little voltage and pH_o sensitivity (Fig. 7 B). The likely formation of a disulfide bond between E363C and L356C by no means proves that residues E363 and L356 normally interact directly. Instead, it reinforces the notion that loosened attachment of the selectivity filter to the surrounding pore helix allows the channel to exhibit pronounced voltage gating, and that, conversely, proper "firm" attachment minimizes voltage gating.

Previously, we showed that the pronounced voltage gating in various E363 mutant channels can be adequately accounted for by a model with four sequentially related states: two closed (C and C_L) and two open (O_1 and O_2) (Martínez-François et al., 2009) (Fig. 11 A). Sequential (multistep) binding of cGMP drives a channel to the final closed state (C_L), whence it may then enter the first open state (O_1). Both transitions are assumed to be voltage insensitive. However, state O_1 is in voltage-sensitive equilibrium with another open state, O_2. In wild-type channels, the voltage-insensitive transition from C_L to O_1 is energetically favored (i.e., high probability), whereas in mutant channels, O_1 is energetically unstable (i.e., low probability) with respect to C_L. Strong depolarization (favoring O_2) will therefore be required to cause a sizeable fraction of channels to open. Assuming for simplicity that only transitions between O_1 and O_2 are voltage sensitive, the relative conductance is then given by:

$$\frac{G}{G_{\max}} = \frac{1}{1+\dfrac{1+\left(\dfrac{K_L}{[cGMP]}\right)^n}{K_1\left(1+K_2 e^{\frac{Z_{K2}FV}{RT}}\right)}}, \quad (1)$$

where $K_L = [C][cGMP]^n/[C_L]$, $K_1 = [O_1]/[C]$, $K_2 = [O_2]/[O_1]$, Z_{K2} is the effective valence associated with the O_1–O_2 transition, V is the membrane voltage, and F, R, and T have their usual meaning.

At saturating concentrations of cGMP, scheme A (Fig. 11 A) reduces to scheme B (Fig. 11 B), and Eq. 1 to

$$\frac{G}{G_{\max}} = \frac{1}{1+\dfrac{1}{K_1\left(1+K_2 e^{\frac{Z_{K2}FV}{RT}}\right)}}. \quad (2)$$

Downloaded from http://rupress.org/jgp/article-pdf/136/2/179/1788741/jgp_201010444.pdf by guest on 11 February 2026

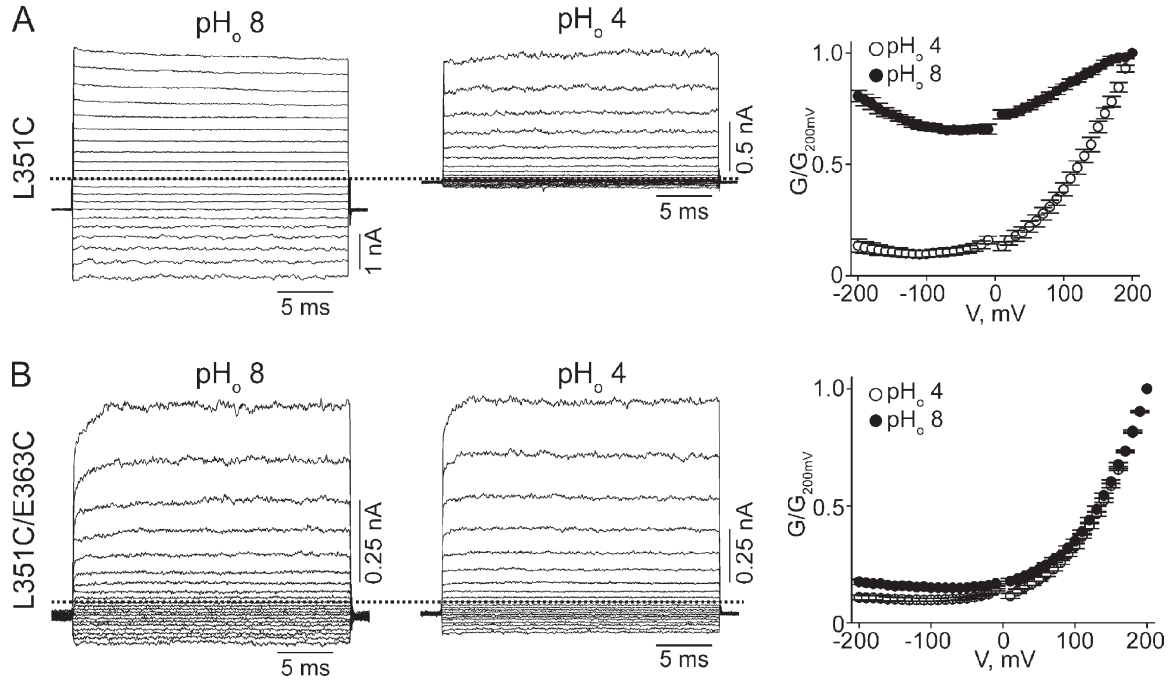

Figure 9. Effects of cysteine mutations at L351 and E363 on proton and voltage sensitivity of CNGA1 channels. (A and B) Macroscopic currents at pH_o 8 (left) or 4 (middle) for the L351C (A) or L351C-E363C (B) mutants, and the corresponding G-V curves (right; mean ± SEM; $n = 5$).

At sufficiently negative voltages, $K_2\exp(Z_{K2}FV/RT)$ vanishes and Eq. 2 reduces to:

$$\frac{G}{G_{\max}} = \frac{1}{1+\frac{1}{K_1}}; \quad (3)$$

that is, K_1 governs the height of the voltage-insensitive, asymptotic plateau at negative voltages. The remaining, voltage-sensitive fraction is described by a Boltzmann function with $V_{1/2} = (RT/Z_{K2}F)\ln[(K_1+1)/K_1K_2]$ and valence Z_{K2}. In the limit where K_1 becomes sufficiently small (i.e., $[O_1]$ is minimal), the conductance plateau at extreme negative voltages vanishes and the conductance becomes voltage gated over its entire range. In such a case, Eq. 2 reduces to a Boltzmann function. The valence Z_{K2} governs the steepness of the G-V curve; K_2 influences only $V_{1/2}$, not the height of the plateau. Because E363 mutations shift the C_L–O_1 equilibrium toward C_L, strong depolarization is required to drive the channels into O_2 to populate open states.

We use the same model to analyze CNGA1's G-V relation at different pH_o. As in the case of E363 mutants, we limit our analysis to the data between 10 and 200 mV because the single-channel i-V curves deviate from linearity at modestly negative voltages (Nizzari et al., 1993; Root and MacKinnon, 1993; Martínez-François et al., 2009). A simultaneous fit of Eq. 2 to the entire dataset yields $K_2 = 0.38 \pm 0.10$ and $Z_{K2} = 0.52 \pm 0.03$ common to all six curves (Fig. 11 C). The values of these two fitted parameters are comparable to those for various mutants with neutral substitutions at E363 (Martínez-François et al., 2009). The fitted K_1 values for each individual pH_o condition are listed in Table I. Fitting a binding isotherm to the relation between K_1 and pH_o yields an apparent pKa of 6.2 (Fig. 11 D). Therefore, like neutral substitutions at E363, protonation of E363 lowers K_1, shifting the C_L–O_1 equilibrium toward C_L. Strong depolarization is then needed to drive the channels toward O_2 to populate open states.

In summary, E363 is critical for proper anchoring of the external end of the selectivity filter of CNGA1 to the pore helix. Neutral mutations at E363 disrupt the anchoring and reveal pronounced voltage gating, as does protonation of the residue. A presumed (engineered) disulfide bond between the external end of the selectivity filter and the pore helix minimizes both extracellular proton sensitivity and voltage gating. Protonation of

TABLE I

Best-fit values of Eq. 2

pH_o	K_1
4	$4.6 \pm 0.9 \times 10^{-2}$
5	$9.7 \pm 1.4 \times 10^{-2}$
6	$4.0 \pm 0.4 \times 10^{-1}$
7	1.1 ± 0.1
8	1.3 ± 0.2
9	1.1 ± 0.1

Downloaded from http://rupress.org/jgp/article-pdf/136/2/179/1788741/jgp_201010444.pdf by guest on 11 February 2026

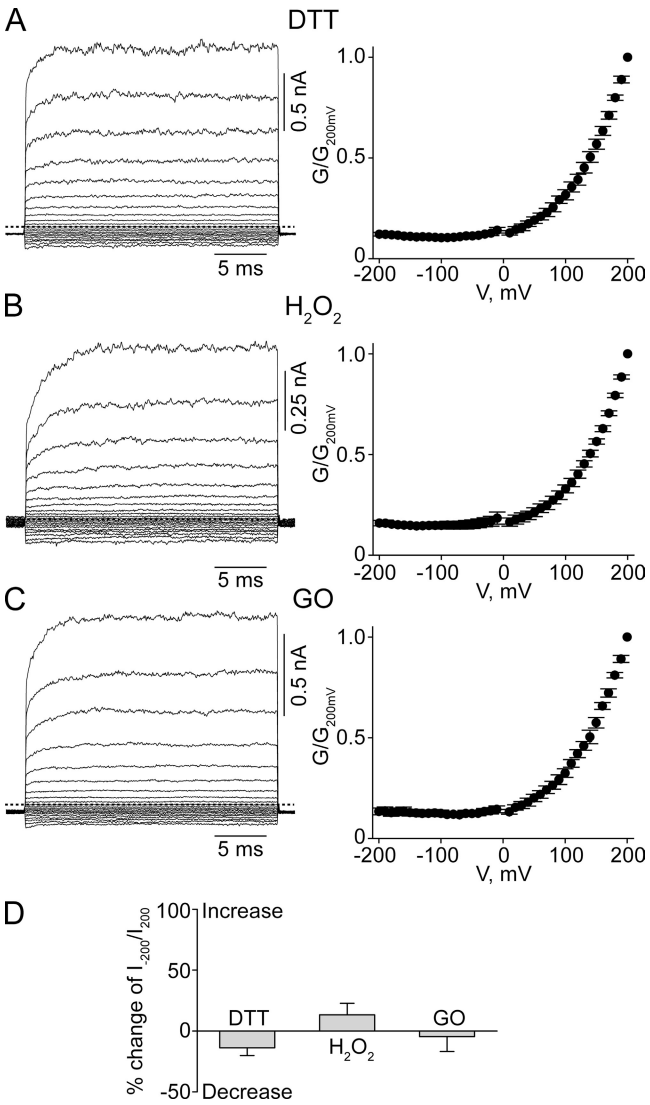

Figure 10. Effects of DTT or H_2O_2 on L351C-E363C double-mutant channels. (A–C) Macroscopic currents at pH_o 8 (left) and corresponding G-V curves (right; mean ± SEM; $n = 5$) for L351C-E363C mutant channels after the application of DTT (A), H_2O_2 (B), or GO (C). (D) Percent change of I_{-200}/I_{200} values (mean ± SEM; $n = 5$) at pH_o 8 of the L351C-E363C double-mutant channels after exposure to the reagents indicated. Positive or negative changes signify increase or decrease in the I_{-200}/I_{200} value, respectively. The changes are not statistically significant (one-way ANOVA) with respect to the control mean.

E363, like substitution of a neutral residue at this position, shifts the gating equilibrium toward closed states, whereas strong depolarization drives the channel from a low probability open state to another open state. Consequently, at low pH_o, the channel open probability exhibits such pronounced voltage sensitivity that channels are practically fully gated by voltage, even in the presence of a saturating concentration of cGMP.

We thank S. Siegelbaum for the CNGA1 channel cDNA clone and P. De Weer for critical review and discussion of our manuscript.

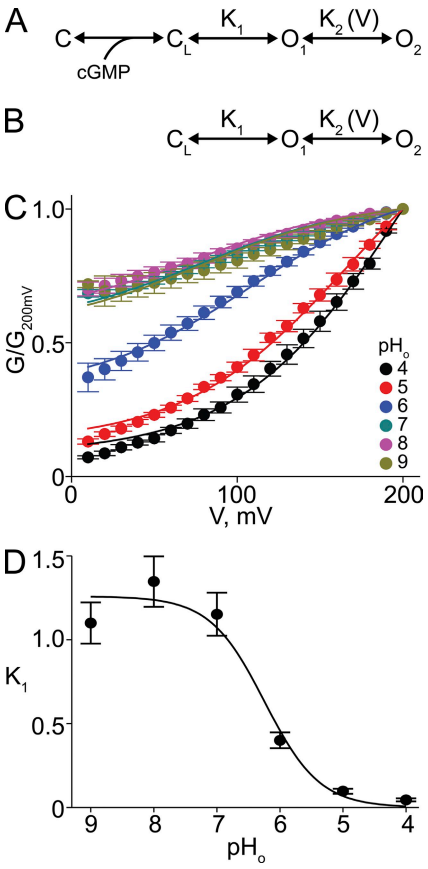

Figure 11. Analysis of voltage gating produced by lowering pH_o. (A and B) Schemes representing gating of the CNGA1 channel, in which C and C_L represent closed channel states without and with cGMP bound, respectively, whereas O_1 and O_2 are two sequential open states in voltage-sensitive equilibrium. (C) Normalized G-V relations (mean ± SEM; $n = 5$) between 10 and 200 mV for CNGA1 channels at the indicated pH_o. Curves correspond to a simultaneous fit of Eq. 2 to all datasets with K_2 and Z_{K2} common to all curves. Best-fit parameters were (common) $K_2 = 0.38 \pm 0.10$ and $Z_{K2} = 0.52 \pm 0.03$, and individual K_1 values at each pH_o (listed in Table I). (D) K_1 plotted against pH_o. Curve is a fit of a binding isotherm yielding apparent pKa = 6.2 ± 0.4.

This study was supported by a grant (GM55560) from the National Institutes of Health to Z. Lu. Z. Lu is an investigator of the Howard Hughes Medical Institute.

Christopher Miller served as editor.

Submitted: 30 March 2010
Accepted: 22 June 2010

REFERENCES

Biel, M., and S. Michalakis. 2009. Cyclic nucleotide-gated channels. *In* cGMP: Generators, Effectors and Therapeutic Implications. H.H.H.W. Schmidt, F. Hofmann, and J.-P. Stasch, editors. Springer, Berlin-Heidelberg. 111–136.

Eismann, E., F. Müller, S.H. Heinemann, and U.B. Kaupp. 1994. A single negative charge within the pore region of a cGMP-gated channel controls rectification, Ca^{2+} blockage, and ionic selectivity. *Proc. Natl. Acad. Sci. USA.* 91:1109–1113. doi:10.1073/pnas.91.3.1109

Fu, Y., and K.W. Yau. 2007. Phototransduction in mouse rods and cones. *Pflugers Arch.* 454:805–819. doi:10.1007/s00424-006-0194-y

Downloaded from http://rupress.org/jgp/article-pdf/136/2/179/1788741/jgp_201010444.pdf by guest on 11 February 2026

Gavazzo, P., C. Picco, and A. Menini. 1997. Mechanisms of modulation by internal protons of cyclic nucleotide-gated channels cloned from sensory receptor cells. *Proc. Biol. Sci.* 264:1157–1165. doi:10.1098/rspb.1997.0160

Goulding, E.H., J. Ngai, R.H. Kramer, S. Colicos, R. Axel, S.A. Siegelbaum, and A. Chess. 1992. Molecular cloning and single-channel properties of the cyclic nucleotide-gated channel from catfish olfactory neurons. *Neuron.* 8:45–58. doi:10.1016/0896-6273(92)90107-O

Guo, D., and Z. Lu. 2000. Pore block versus intrinsic gating in the mechanism of inward rectification in strongly rectifying IRK1 channels. *J. Gen. Physiol.* 116:561–568. doi:10.1085/jgp.116.4.561

Guo, D., and Z. Lu. 2002. IRK1 inward rectifier K^+ channels exhibit no intrinsic rectification. *J. Gen. Physiol.* 120:539–551. doi:10.1085/jgp.20028623

Jencks, W.P. 1987. Catalysis in Chemistry and Enzymology. Dover Publications Inc., New York. 864 pp.

Kaupp, U.B., and R. Seifert. 2002. Cyclic nucleotide-gated ion channels. *Physiol. Rev.* 82:769–824.

Kaupp, U.B., T. Niidome, T. Tanabe, S. Terada, W. Bönigk, W. Stühmer, N.J. Cook, K. Kangawa, H. Matsuo, T. Hirose, et al. 1989. Primary structure and functional expression from complementary DNA of the rod photoreceptor cyclic GMP-gated channel. *Nature.* 342:762–766. doi:10.1038/342762a0

Liman, E.R., J. Tytgat, and P. Hess. 1992. Subunit stoichiometry of a mammalian K^+ channel determined by construction of multimeric cDNAs. *Neuron.* 9:861–871. doi:10.1016/0896-6273(92)90239-A

Long, S.B., X. Tao, E.B. Campbell, and R. MacKinnon. 2007. Atomic structure of a voltage-dependent K^+ channel in a lipid membrane-like environment. *Nature.* 450:376–382. doi:10.1038/nature06265

Lu, Z., and R. MacKinnon. 1995. Probing a potassium channel pore with an engineered protonatable site. *Biochemistry.* 34:13133–13138. doi:10.1021/bi00040a026

Martínez-François, J.R., Y. Xu, and Z. Lu. 2009. Mutations reveal voltage gating of CNGA1 channels in saturating cGMP. *J. Gen. Physiol.* 134:151–164. doi:10.1085/jgp.200910240

Matulef, K., and W.N. Zagotta. 2003. Cyclic nucleotide-gated ion channels. *Annu. Rev. Cell Dev. Biol.* 19:23–44. doi:10.1146/annurev.cellbio.19.110701.154854

Mazzolini, M., C. Anselmi, and V. Torre. 2009. The analysis of desensitizing CNGA1 channels reveals molecular interactions essential for normal gating. *J. Gen. Physiol.* 133:375–386. doi:10.1085/jgp.200810157

Nizzari, M., F. Sesti, M.T. Giraudo, C. Virginio, A. Cattaneo, and V. Torre. 1993. Single-channel properties of cloned cGMP-activated channels from retinal rods. *Proc. Biol. Sci.* 254:69–74. doi:10.1098/rspb.1993.0128

Picco, C., C. Sanfilippo, P. Gavazzo, and A. Menini. 1996. Modulation by internal protons of native cyclic nucleotide–gated channels from retinal rods. *J. Gen. Physiol.* 108:265–276. doi:10.1085/jgp.108.4.265

Root, M.J., and R. MacKinnon. 1993. Identification of an external divalent cation-binding site in the pore of a cGMP-activated channel. *Neuron.* 11:459–466. doi:10.1016/0896-6273(93)90150-P

Root, M.J., and R. MacKinnon. 1994. Two identical noninteracting sites in an ion channel revealed by proton transfer. *Science.* 265:1852–1856. doi:10.1126/science.7522344

Sesti, F., E. Eismann, U.B. Kaupp, M. Nizzari, and V. Torre. 1995. The multi-ion nature of the cGMP-gated channel from vertebrate rods. *J. Physiol.* 487:17–36.

Stryer, L. 1986. Cyclic GMP cascade of vision. *Annu. Rev. Neurosci.* 9:87–119. doi:10.1146/annurev.ne.09.030186.000511

Yau, K.W., and D.A. Baylor. 1989. Cyclic GMP-activated conductance of retinal photoreceptor cells. *Annu. Rev. Neurosci.* 12:289–327. doi:10.1146/annurev.ne.12.030189.001445

Downloaded from http://rupress.org/jgp/article-pdf/136/2/179/1788741/jgp_201010444.pdf by guest on 11 February 2026